

**PRELIMINARY CHARACTERIZATION OF SPINEL TROCTOLITE CLAST IDENTIFIED IN APOLLO NEXT GENERATION SAMPLE ANALYSIS (ANGSA) CORE 73002.** A. C. Stadermann<sup>1</sup>, J. Gross<sup>1,2,3,4</sup>, T. M. Erickson<sup>5</sup>, J. J. Barnes<sup>6</sup>, S. A. Eckley<sup>5</sup>, F. M. McCubbin<sup>1</sup>, and the ANGSA Science Team<sup>7</sup>, <sup>1</sup>ARES, NASA Johnson Space Center, Houston, TX (amanda.c.stadermann@nasa.gov), <sup>2</sup>Rutgers, The State University of New Jersey, Piscataway, NJ; <sup>3</sup>American Museum of Natural History, New York, NY 10024; <sup>4</sup>Lunar and Planetary Institute, Houston, TX 77058; <sup>5</sup>Jacobs-JETS, NASA Johnson Space Center, Houston, TX, <sup>6</sup>Lunar and Planetary Laboratory, University of Arizona, Tucson, AZ, <sup>7</sup>List of co-authors includes all members of the ANGSA Science team (<https://www.lpi.usra.edu/ANGSA/teams/>).

**Introduction:** The lunar magnesian (Mg-) suite is a diverse lithological group composed of Mg-rich mafic minerals [1,2]. The Mg-suite consists primarily of troctolites, norites, gabbronorites, and spinel troctolites. These rocks exhibit contradictory geochemical traits, with mafic minerals bearing high Mg# (molar  $100 \times \text{Mg}/[\text{Mg}+\text{Fe}]$ ) indicating primitive parental magmas, but also plagioclase saturation and enrichments in incompatible trace elements (i.e., KREEP) indicate more evolved parental magmas. A variety of models have been invoked to explain the occurrence and petrogenesis of the Mg-suite [2–4].

Here, we report on a new spinel troctolite clast found in Apollo Next Generation Sample Analysis (ANGSA) program core 73002. Sample 73002 was acquired at Station 3 during Apollo 17 as the upper part of a double-drive tube with sample 73001. During processing, the spinel troctolite clast (0.066 g) was found at the 4.0–4.5 cm depth interval.

**Methods:** We have obtained X-ray computed tomography (XCT) data, backscattered electron (BSE) images, energy dispersive x-ray spectroscopy (EDS) maps, electron probe microanalysis (EPMA) data, and electron backscatter diffraction (EBSD) maps of this clast and its prepared section. Here we present a subset of these data.

We obtained a large-area EBSD map of the section (spanning a rectangular area approximately  $1.7 \times 2.2$  mm) with a spatial resolution of  $1 \mu\text{m}$ , in addition to smaller, higher-resolution maps of regions of interest (up to  $0.05 \mu\text{m}$  spatial resolution). EPMA analyses were carried out with a focused beam ( $<1 \mu\text{m}$ ) and defocused beam ( $5 \mu\text{m}$  for plagioclase analyses), 20 nA beam current, and 15 keV acceleration voltage.

**Results & Discussion:** Spinel troctolite 73002,456 contains plagioclase, olivine, Mg-Al-spinel, orthopyroxene, and clinopyroxene (Fig. 1). Using EDS maps,

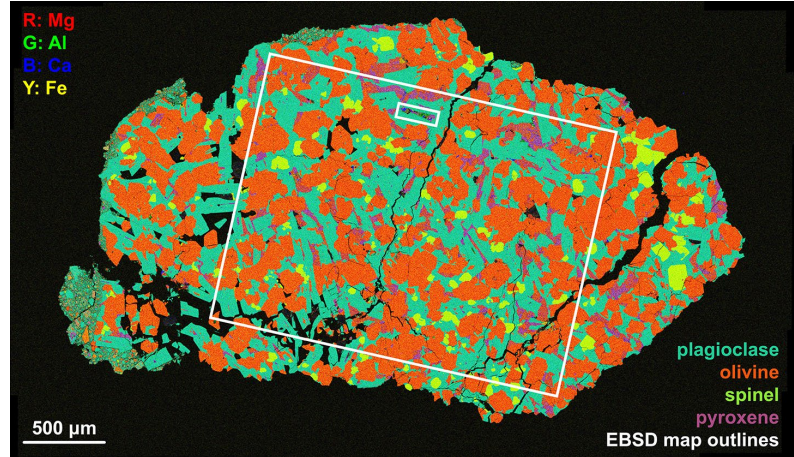


**Figure 1.** Energy dispersive X-ray spectroscopy (EDS) map of spinel troctolite 73002,456, showing Mg in red, Al in green, Ca in blue, and Fe in yellow. This color scheme reveals plagioclase in green-teal, olivine in red-orange, spinel in green-yellow, pyroxene in red-purple. Locations of EBSD maps are highlighted in white outlines.

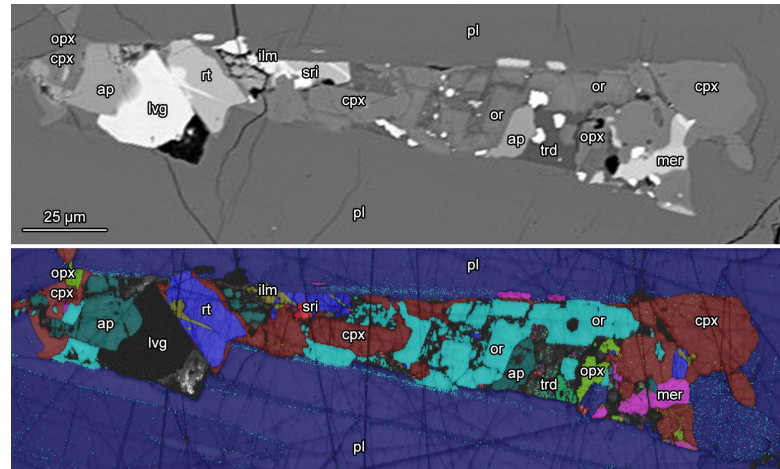


**Figure 2.** Top: BSE image of a large mesostasis region outlined in Figure 1. Bottom: EBSD phase map of same region. Phase abbreviations: opx: orthopyroxene; cpx: clinopyroxene; ap: apatite; lvg: loveringite; rt: rutile; ilm: ilmenite; sri: srilankite; pl: plagioclase; or: orthoclase; trd: tridymite; mer: merrillite.

we determined phase abundances of 40.3% plagioclase, 39.1% olivine, 15.3% pyroxene (undivided), and 4.6% spinel. Plagioclase crystals partially enclose the olivine and spinel crystals. The grains are up to  $200 \mu\text{m}$  in size and range in composition from  $\text{An}_{94}\text{Ab}_5\text{Or}_1$  in the core and increase in Ab content towards the rim to  $\text{An}_{80}\text{Ab}_{17}\text{Or}_3$ . A rare orthoclase is also observed in an interstitial pocket (Fig. 2) that contains 3.97 wt. % BaO

with a composition of  $An_{2.7}Ab_{0.5}Or_{89.3}Cn_{7.5}$ . The olivine grains are subhedral and up to 230  $\mu\text{m}$  in size. Compositionally the grains are homogeneous ranging from  $FO_{89-86}$ . Interstitial pyroxenes exhibit irregular exsolution and range in composition from  $Wo_{46-3}En_{83-46}Fe_{17-6}$  with a Mg# of 82–89. Spinel grains are generally euhedral to subhedral, up to 150  $\mu\text{m}$  in size, and have an average composition of  $Cr_6Sp_{94}Ul_{v1}$ . The Cr# (molar  $100 \times Cr/[Cr+Al]$ ) ranges from Cr# 8–4 and the Fe# (molar  $100 \times Fe/[Fe+Mg]$ ) ranges from Fe# 26–19. Some euhedral spinel grains contain inclusions of small euhedral olivine grains (Fig. 3). However, some spinel grains are anhedral and exhibit resorption features at their rims with submicron exsolution lamellae in their core regions (too small to determine their composition). The resorption features are enriched in Cr with a composition of  $Cr_{10-12}Sp_{90-87}Ul_{v0-1}$  (Fig. 3). The olivine, spinel, and pyroxene exhibit no crystallographic preferred orientation, but plagioclase has a moderate crystallographic preferred orientation (Fig. 4).

Trace phases include orthoclase, ilmenite, merrillite, apatite, rutile, zirconolite, baddeleyite, srilankite, silica, loveringite, troilite, and metal (Fig. 2). We believe the identification of srilankite (orthorhombic  $ZrTi_2O_6$ ) in 73002,456 to be the first reporting of this mineral in a lunar sample. We identify a phase geochemically consistent with loveringite,  $Ca(Ti,Fe,Cr,Mg,Zr,Al,REE)_{21}O_{38}$ , but which does not diffract under the electron beam for EBSD, implying it is not crystalline. Loveringite, a hexagonal Ti-Fe-Cr-Zr-Ca oxide, has been historically reported as “Cr-Zr-Ca armalcolite,” which is orthorhombic [5,6].

Spinel troctolite 73002,456 is geochemically and petrographically

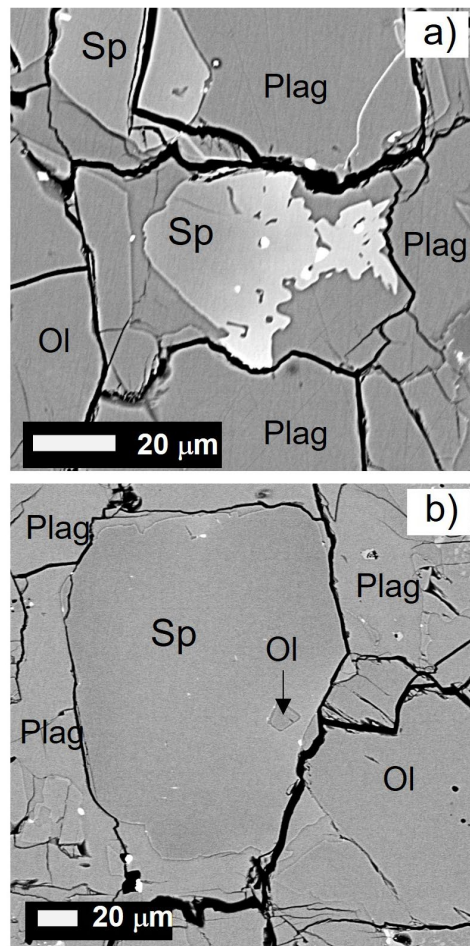


**Figure 3.** Backscattered electron (BSE) images of 73002,456. (a) Spinel with resorption features at right side of grain. (b) Spinel with enclosed euhedral olivine.

similar to previously reported spinel troctolites [7,8], although plagioclase extends to more Na-rich compositions in this clast.

**Conclusions & Future Work:** We have characterized this spinel troctolite clast using a variety of electron beam techniques, and plan to further assess the volatile inventory held within apatite in this sample.

**Acknowledgements:** We thank NASA for the loan of Apollo sample 73002,456. ACS acknowledges support from a NASA Postdoctoral Program (NPP) Fellowship, administered by Oak Ridge Associated Universities. JG acknowledges grant #80NSSC19K0558 and JJB acknowledges grant #80NSSC19K0803.

**References:** [1] James, O. B. (1980) *LPS XI* 365-393. [2] Shearer C. K. et al. (2015) *Am. Min.* 100(1). [3] Elardo S. M. et al. (2011) *GCA* 75(11). [4] Prissel T. C. and Gross J. (2020) *EPSL* 511. [5] Săbău G. and Alberico A. (2007) *SUBB Geologica* 52. [6] Zhang A.-C. et al. (2020) *Am. Min.* 105(7). [7] Prinz M. et al. (1973) *Science* 179(4068). [8] Gross J. and Treiman A. H. (2011) *JGR: Planets* 116(E10).

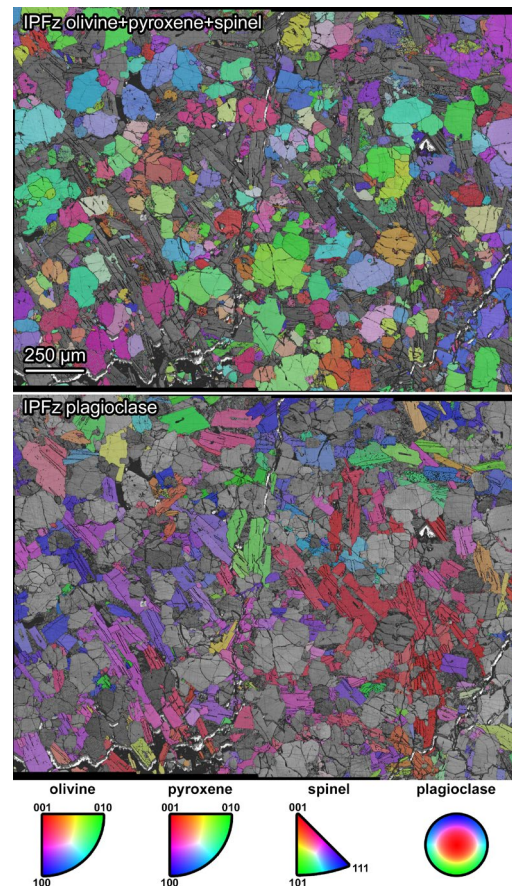


**Figure 4.** Large-area EBSD maps of 73002,456. Top: Inverse pole figure (IPF)<sub>z</sub> map showing olivine, pyroxene, and spinel, each with no crystallographic preferred orientation. Bottom: IPF map showing plagioclase with moderate crystallographic preferred orientation.